

# Comparative assessment of two portable Raman spectrometers for the characterisation of historical natural dye lakes

Silvia Bottura-Scardina<sup>1</sup>  | Peter Vandennebeele<sup>2,3</sup>  | Catarina Miguel<sup>1,4</sup>  | António Candeias<sup>1,4</sup> 

<sup>1</sup>HERCULES Laboratory, Institute for Advanced Studies and Research, University of Évora, Largo Marquês de Marialva 8, Évora, Évora, 7000-809, Portugal

<sup>2</sup>Raman Spectroscopy Research Group, Department of Analytical Chemistry, Ghent University, Krijgslaan 281, Ghent, Ghent, B-9000, Belgium

<sup>3</sup>Archaeometry Research Group, Department of Archaeology, Ghent University, Sint-Pietersnieuwstraat 35, Ghent, Ghent, B-9000, Belgium

<sup>4</sup>City University of Macau Chair in Sustainable Heritage, University of Évora, Rua Dom Augusto Eduardo Nunes 2, Évora, Évora, 7000-651, Portugal

## Correspondence

Silvia Bottura-Scardina, HERCULES Laboratory, Institute for Advanced Studies and Research, University of Évora, Largo Marquês de Marialva 8, 7000-809 Évora, Portugal.

Email: [scardina@uevora.pt](mailto:scardina@uevora.pt)

## Funding information

Cistercian Horizons, Grant/Award Number: PTDC/ART-HIS/29522/2017; Portuguese Foundation for Science and Technology; HERCULES Laboratory, Grant/Award Numbers: UIDB/04449/2020, UIDP/04449/2020; Norma Transitória, Grant/Award Number: DL 57/2016/CP1372/CT0012

## Abstract

This paper explores the use of portable Raman instruments to characterise natural dye lakes in paint mixtures, as an alternative approach to other Raman techniques (e.g. SERS). Raman spectroscopy has indeed been used extensively to study natural dyes as pure substances or as artistic pigments (dye lakes). However, the examination of these compounds with Raman spectroscopy is particularly challenging because of a strong fluorescence, a relatively weak Raman signal and their occurrence at low concentrations in artefacts. Because of these challenges, the typical way of analysing these materials is through either surface-enhanced Raman spectroscopy (SERS) or Fourier-transform (FT) Raman spectroscopy, yet those approaches are not always desirable in art analysis, especially as they often require micro-sampling. Therefore, this study explores the potential of using commercial mobile instruments, which would open the possibilities for direct *in situ* analysis. Two dispersive instruments, one using a fibre-optic probe and a 1064-nm excitation laser and the other using the subtracted-shifted excitation (SSE) post-processing algorithm, have been tested in their feasibility to characterise dye lakes. Raman spectra were acquired from a set of laboratory reproductions of paint mixtures prepared with a chosen set of common lakes, three red (brazilwood, cochineal and madder) and one yellow (weld), mixed with natural proteinaceous and polysaccharide binders. The feasibility has been evaluated, and it is shown that these lakes produce a detectable Raman signal, in spite of the strong interference of the painting support (parchment) and that the two instruments provide significantly different information.

## KEYWORDS

brazilwood, cochineal, dye analysis, madder, mobile Raman instrumentation

This is an open access article under the terms of the [Creative Commons Attribution-NonCommercial-NoDerivs](https://creativecommons.org/licenses/by-nc-nd/4.0/) License, which permits use and distribution in any medium, provided the original work is properly cited, the use is non-commercial and no modifications or adaptations are made.

© 2023 The Authors. *Journal of Raman Spectroscopy* published by John Wiley & Sons Ltd.

## 1 | INTRODUCTION

A major challenge for conservation scientists is the identification of historical organic dyes in painted artworks. These encompass the dyestuffs derived from such natural sources as animal and plant juices, which were typically further processed prior to pictorial use. Because of their strong solubility in the aqueous medium, natural dyes are not suitable for direct use and need to be converted to a water-insoluble form, for instance through precipitation as an insoluble metal-dye complex,<sup>[1–3]</sup> with alum ( $\text{KAl}[\text{SO}_4]_2 \cdot 12 \text{H}_2\text{O}$ ) being the predominant choice to obtain  $\text{Al}^{3+}$  and form the Al (III)-chelates.<sup>[4–6]</sup> These complexes are commonly named *lakes* and found large use in painted artefacts like easel paintings<sup>[7]</sup>, print colouring<sup>[8,9]</sup> or illuminated manuscripts.<sup>[10–12]</sup>

To detect historical lakes' composition, Raman spectroscopy has proved to be a useful method, yet with some challenges. Lakes typically contain molecules with a large absorption cross-section of visible radiation like hydroxyanthraquinones, homoisoflavonoids, flavonols or indigoids,<sup>[13,14]</sup> and consequently, their tinting strength is very high. As a result, these materials generally occur at low concentrations in artefacts.<sup>[15]</sup> Another factor is that some dyes are strongly fluorescent in the visible range,<sup>[14,16,17]</sup> resulting in a dominating fluorescence background that obscures their Raman signal. Moreover, in artworks, Raman features can also be overwhelmed by the interfering fluorescence of other materials present like binders and extenders in the same matrix, of other pictorial levels or even of the painting support.

Some strategies have been elaborated to work around these challenges. The most common approach is to amplify the Raman cross-section by adsorbing a small portion of these materials on metal surfaces (surface-enhanced Raman spectroscopy, SERS; surface-enhanced resonance Raman spectroscopy, SERRS) that allowed to obtain Raman spectra of several major chromophores in their pure form, including alizarin,<sup>[18–21]</sup> purpurin,<sup>[20,21]</sup> carminic acid,<sup>[20,22]</sup> laccaic acid,<sup>[20,23]</sup> indigo,<sup>[15]</sup> luteolin and apigenin.<sup>[24,25]</sup> Fourier-transform Raman spectroscopy (FT-Raman spectroscopy) is another approach to reduce the interference from fluorescence, that is, however, less frequently used. However, it was implemented to characterise alizarin,<sup>[18]</sup> chrysin, apigenin, luteolin<sup>[26]</sup> and brazilein—either pure<sup>[27]</sup> or in association with other compounds from wood samples.<sup>[28]</sup>

Not only individual natural dyes but also their coordination complexes have been investigated with Raman methods. In some cases, those studies involved laboratory reproductions<sup>[29–31]</sup>; other times, they were characterised with subtracted-shifted Raman microscopy,<sup>[32–36]</sup> FT-Raman spectroscopy,<sup>[37]</sup> SERRS<sup>[38,39]</sup> and SERS the red lakes of historical textile<sup>[40–44]</sup> or paint<sup>[45,46]</sup> samples.

Yellow and blue lakes have also been studied through SERS<sup>[42,47]</sup> or SERS-derived techniques.<sup>[50]</sup>

Although efficient, the mentioned methods present several drawbacks. The most apparent is that analysing with benchtop instruments requires either displacing the artwork bearing the dye lake-containing paints to an analytical facility or micro-sampling the materials of interest. Moreover, specific training is needed to prepare the SERS substrates to examine the dye. In general, in cultural heritage research, sample-based techniques are not desirable as they cause micro-destruction of the artefact under study. As the collected samples typically cannot be recovered from the SERS surfaces, they are not available for further analysis. Finally, one or more stages of sample preparation can be necessary, reducing the advantages of Raman spectroscopy.

Portable Raman methods offer an interesting alternative. Relatively low-weight instrumentation can be carried around to inspect an artistic object on its site of conservation.<sup>[51]</sup> Adopting portable devices allows minimising the threat of mechanical and chemical micro-damage caused by dislocation while avoiding the need of micro-sampling. These opportunities encouraged archaeometric applications of the technique<sup>[52–57]</sup>; thus, a variety of artistic objects was characterised in field surveys with mobile instruments: amongst others, stained glasses,<sup>[58,59]</sup> glazed ceramic artefacts<sup>[60–64]</sup> or illuminated manuscripts.<sup>[65,66]</sup>

The growing popularity of portable Raman methods for art technical examinations motivated closer attention to challenge their adequacy to lake analysis through this paper. More specifically, this study evaluates two commercial portable Raman instruments. One is a dispersive spectrometer equipped with a near-infrared laser (1064 nm), and the other instrument uses subtracted-shifted excitation (SSE) Raman spectroscopy<sup>[67,68]</sup> to eliminate the fluorescence. The infrared instrument in this study uses a fibre-optics probe to focus the laser beam, while using the SSE device, the beam is directly focussed on the artwork, and the spectrometer head has to touch the artwork for optimal results.

This study considers a set of accurate historical paint reproductions of widely studied lakes (madder, cochineal, brazilwood and weld), all prepared according to the instructions of technical texts on book illumination from the 12th–16th century. This choice was driven by two major reasons: one is that the pictorial stratigraphy of book illumination is relatively simplified when compared with other painting techniques. The other is that *in situ* measurements of these mixtures are heavily affected by the fluorescence arising from the parchment support. The current work aims at addressing four major points: (i) to evaluate the ability of portable instruments to detect the main chromophores of lakes, (ii) to discriminate the

binding media, (iii) to evaluate the spectral information contributed by each portable approach and (iv) to assess the spectral differences between these methods and micro-invasive techniques (SERS and FT-Raman spectroscopy) that are extensively described in previous studies.

## 2 | EXPERIMENTAL

### 2.1 | Samples

The materials for the reproductions were all prepared from raw materials purchased from Kremer-Pigmente

GmbH & Co., Germany, and they are presented in Table 1. The mixtures for the paint models were applied directly on parchment sheets (no preparatory layer) as  $1.5 \times 1.5$  cm squares, with a dye lake-to-binder ratio fixed to 1:4 (wt:wt, dry weight).

The chosen set of lakes contains dyes with a well-documented chemical structure. The natural precursors never contain a single chromophore, but rather a mixture of compounds, as demonstrated by chromatographic characterisations. These studies further proved that dyes may occur as residual glycosides, aside from their free (aglycone) form,<sup>[69,70]</sup> at rates depending on the conditions of lake preparation and on the composition of

TABLE 1 List of the materials used for the preparation of the laboratory mock-ups

Class	Material	Supplier	Kremer reference code
Dyes	Brazilwood, shavings	Kremer-Pigmente	#36150
	Cochineal, dried scale insects	Kremer-Pigmente	#36040
	Madder, roots	Kremer-Pigmente	#37201
	Weld, <i>Reseda luteola</i> L. dried plant	Kremer-Pigmente	#36250
Binders	Egg white	Biological hen eggs, local supplier	-
	Egg yolk	Biological hen eggs, local supplier	-
	Gum Arabic, pieces of dry exudate	Kremer-Pigmente	# 63300
Support	Parchment, artisanal	Musée du Parchemin (Rouen, France)	-

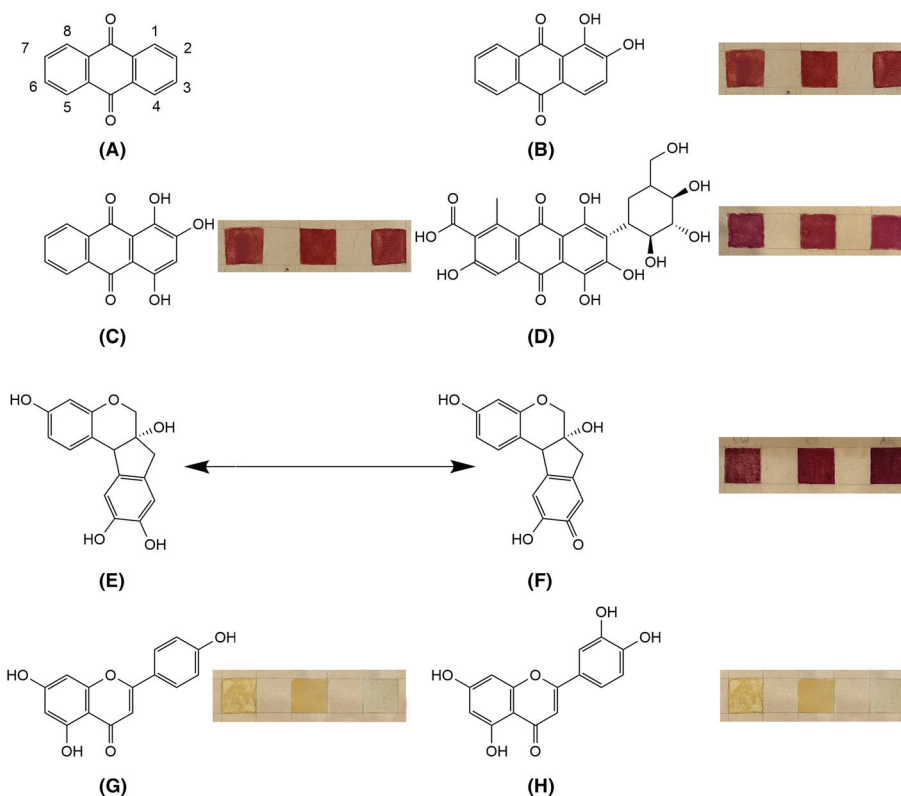


FIGURE 1 Major chromophores and backbones found in the considered lakes: (A) anthraquinone, (B) alizarin, (C) purpurin, (D) carminic acid, (E) brazilein, (F) brazilein, (G) apigenin and (H) luteolin. The images at the right of (A) and (B) represent the mock-ups of madder lake mixed with egg white, gum Arabic and yolk (from left to right); that right to (C) represents the mock-ups of cochineal lake mixed to the same binders and before; the image right to (F) represents the mock-ups of brazilwood lake; the images right to (G) and (H) represent the mock-ups of weld lake.

the natural precursors. Two of the considered red lakes (madder and cochineal) have chromophores of the anthraquinone class: their main structure is an anthraquinone (9,10-anthracenedione) (Figure 1A) to which methyl-, carboxy-, hydroxyl-, glucosidal or other aliphatic groups are attached (Figure 1B–D). The chromophore for the other red lake (brazilwood) is a homoisoflavonoid of the brazilin type that has two tautomeric forms (Figure 1E,F). The yellow lake (weld) under study contains two hydroxyflavones (Figure 1G,H).

## 2.2 | Instrumentation

Part of the Raman spectra was recorded with a dispersive, laptop-controlled fibre-optic portable Raman spectrometer i-Raman<sup>®</sup> EX by B&W Tek (Newark, USA). The spectrometer is coupled with a 1064-nm excitation laser and a TE-cooled InGaAs detector, and it is able to record spectra from 100 to 2500  $\text{cm}^{-1}$  with a spectral resolution of  $<10.0 \text{ cm}^{-1}$  (at 1296 nm). The fibre-optics probe was fixed to the BAC150B XYZ stage (B&W Tek) for short-distance measurements. The laser power was adapted to ensure that no detector saturation occurred, nor that material was ablated, and a good signal-to-noise ratio (S/N) was achieved. Typical measurement conditions were 30-s integration time, 10 accumulations and 60% laser power (approximately 70 mW at the sample). Data collection was performed with BWSpec (v.4.10\_4) software, using a USB 2.0 connection between the spectrometer and laptop computer. The dark spectra and calibration standards were recorded individually to allow for spectral post-processing with MATLAB R2022b (spectral averaging of 10 accumulations, dark subtraction, wavenumber calibration, polynomial baseline correction, smoothing). The wavenumber calibration was based on the main bands of sulfur, caprolactone, acetonitrile/toluene (50/50, v/v) and polystyrene<sup>[71]</sup>; baseline subtraction was performed by iteratively fitting a third-degree polynomial function; and the spectra were slightly smoothed using a smoothing spline with  $p$  coefficient adjusted between 0.004 and 0.051.

Other Raman spectra were recorded with a Bruker BRAVO (Ettlingen, Germany) handheld Raman instrument. The spectrometer is coupled with two excitation lasers (785 and 853 nm) and a CCD detector, allowing for a spectral range between 300 and 3200  $\text{cm}^{-1}$  with a resolution of 10–12  $\text{cm}^{-1}$ . The system has a fixed laser power of less than 100 mW at the sample. For the analysis, the sample sheet was mounted vertically in front of the device that was placed on a laboratory lift platform, allowing to adjust the height according to the need. Data were typically recorded with 10- to 50-s

integration time. The software records for each laser three different spectra with slightly different excitation wavelengths, and by using the shifted wavelength spectral subtraction algorithm, the background-corrected Raman spectra are reconstructed.

## 3 | RESULTS AND DISCUSSION

### 3.1 | Identification of the lake chromophores

Baseline-corrected Raman spectra of the lakes under investigation revealed the constant presence of some characteristic bands for each class of compounds (Figures 2 and 3), all being prepared according to traditional recipes with respect to both lake synthesis and paint formulation, and applied on parchment. A spectrum of the blank parchment has been added at the bottom of the figures for clarity (Figures 2D and 3B).

At first sight of the Raman spectra of laboratory reproductions, they showed that the most distinct information was in those recorded with the fibre-optic instrument. These latter spectra show more features than the others, with the only challenge that some bands that can be associated with the collagen of the parchment support are also

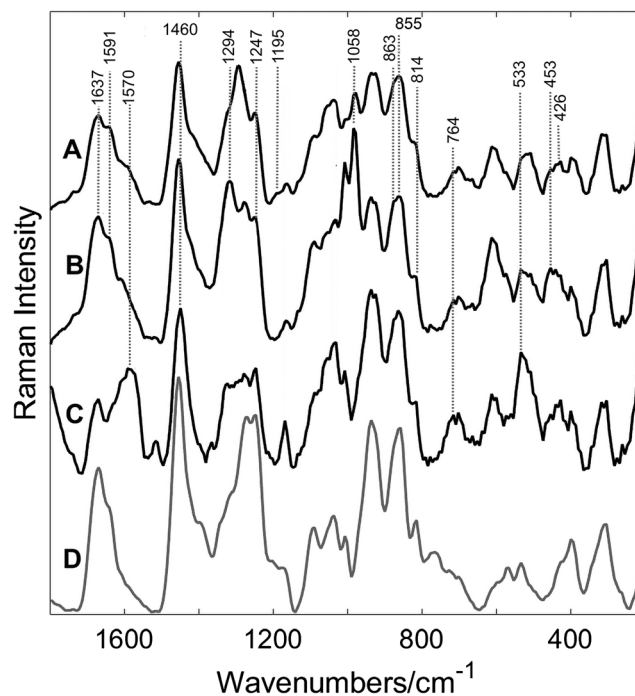


**FIGURE 2** Raman spectra of red dye mock-ups (mixed in gum Arabic), all excited with 1064-nm laser, 10 accumulations, 30-s integration time and captured with the fibre-optic instrument: (A) madder lake, (B) cochineal lake, (C) brazilwood lake and (D) parchment ground. Raman band positions ( $\text{cm}^{-1}$ ) are marked as discussed in the text.

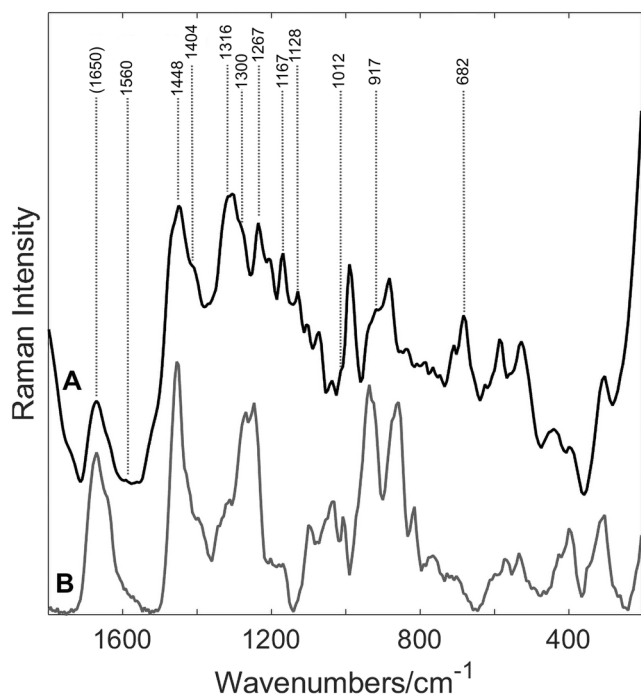


**FIGURE 3** Raman spectra of the yellow dye mock-ups (mixed in gum Arabic), all excited with 1064-nm laser, 10 accumulations, 30-s integration time and captured with the fibre-optic instrument. Raman band positions ( $\text{cm}^{-1}$ ) are marked as discussed in the text. The band at  $1650\text{ cm}^{-1}$  is put between brackets because it could either come from the parchment support or several stretching modes of the chromophore luteolin (compare with Table 3).

observed (Figure 2D), starting from the red lakes model (Figure 2 and Table 2). In fact, amide I and III features around  $1650$  and  $1250\text{ cm}^{-1}$  are clearly observed, and the  $\delta$  (CH) bending vibrations yield an intense Raman band around  $1550\text{ cm}^{-1}$ . Amide modes are characteristic of proteinaceous materials like parchment as well as protein-based binding agents used in illumination, namely glair-denatured hen egg white. Together with the mentioned bands, two more intense features are present in the region between  $1000$  and  $800\text{ cm}^{-1}$ , where occur vibrational modes associated  $\nu$  (CO) and  $\nu$  (CC) stretching modes as  $\rho$  ( $\text{CH}_3$ ) and  $\rho$  ( $\text{CH}_2$ ) deformations. Despite these Raman bands of the support—and probably the binder—being present in the spectra, characteristic Raman features of the lakes can still be detected clearly.

At the low wavenumber shoulder of the amide I band ( $\nu$  [CONH]), some of those peculiar features are observed. Madder lake-based paints show a weak Raman band at  $1637\text{ cm}^{-1}$  from the  $\nu$  (C=O) stretching vibration of the carbonyl groups of the anthraquinone backbone<sup>[35]</sup> and at  $1591\text{ cm}^{-1}$  assigned to the  $\nu$  (CC) of alizarin and purpurin.<sup>[19,35]</sup> In cochineal lake-based paints, the bands are slightly higher in wavenumber (shifting from  $1637$  to  $1639\text{ cm}^{-1}$ ) and have been assigned to the  $\nu$  (CO) and

$\nu$  (CC) stretching vibrations of carminic acid.<sup>[22]</sup> In the Raman spectrum of the historical reproductions of brazilwood lake, an intense feature is observed around  $1570\text{ cm}^{-1}$ . It shows different overlapping Raman bands, understood as the  $\nu$  (C=C) and  $\nu$  (C=O) stretching vibrations of both tautomeric forms of brazilin.<sup>[27,44]</sup>

In the region between the parchment's  $\delta$  (CH) bending vibration (approximately  $1450\text{ cm}^{-1}$ ) and the amide III band (approximately  $1250\text{ cm}^{-1}$ ), several overlapping Raman bands are observed, all associated with  $\delta$  (CH) bending vibrations and  $\nu$  (CC) stretching vibrations of the chromophores.<sup>[19,35,71]</sup> As to the anthraquinoid lakes, the most intense band of those of cochineal is slightly upshifted (approximately  $1320\text{ cm}^{-1}$ ) when compared with those of madder (approximately  $1290\text{ cm}^{-1}$ )<sup>[22]</sup>; the Raman spectra of brazilwood lake display a broader massif of overlapping Raman bands in the same spectral region.<sup>[27]</sup> Between approximately  $1000$  and  $1450\text{ cm}^{-1}$ , the spectra of red lakes reveal combinations of stretching with bending modes, including aromatic ring vibrations. Indeed, the bands at approximately  $1460$ ,<sup>[19,72]</sup>  $1294$ ,<sup>[19,35]</sup>  $1247$ <sup>[19]</sup> and  $1195\text{ cm}^{-1}$ <sup>[19,35]</sup> of madder lakes have been reported in literature of alizarin and purpurin, and they could arise from the anthraquinone backbone and the hydroxyl functional groups attached between the C1–C4 positions. In the cochineal lake samples, two significant bands are observed at approximately  $855$  and  $1058\text{ cm}^{-1}$ , being assigned to the Glu and  $\delta$  ( $\text{CH}_3$ ) deformations of the glucitol and methyl functions of carminic acid.<sup>[22]</sup> Similarly, the mock-ups of brazilwood lake show a series of bands characteristic of the chromophore brazilin, namely those at approximately  $1241$ <sup>[27]</sup> and  $1168\text{ cm}^{-1}$ <sup>[27]</sup>; those at  $1310$ ,  $1294$  and  $1272\text{ cm}^{-1}$  are attributed to  $\nu$  (C–O),  $\nu$  (C–C) and  $\delta$  ( $\text{CH}_2$ ) vibrations.<sup>[27]</sup>

The spectral region between  $700$  and  $900\text{ cm}^{-1}$  contains  $\delta$  (C–O) and  $\delta$  (C–H) bending modes of aliphatic substituents and hydroxyl groups ( $850$ – $863\text{ cm}^{-1}$  for alizarin and purpurin,<sup>[19,35]</sup>  $814$ – $820\text{ cm}^{-1}$  for carminic acid<sup>[22]</sup> and  $764\text{ cm}^{-1}$  for brazilin).<sup>[44]</sup> The region between  $400$  and  $600\text{ cm}^{-1}$  reveals two broad features consisting of several overlapping Raman bands, all attributed to skeletal deformations. Especially while inspecting madder lake and cochineal, a clear band centred around  $453\text{ cm}^{-1}$  is observed in the latter spectrum.

The Raman spectra of the weld yellow lake considered in this study also revealed a set of characteristic bands (Figure 3), which are listed in Table 3. The  $\nu$  (C=O) stretching vibrations of apigenin and luteolin are expected in the spectral region around  $1650\text{ cm}^{-1}$ , but these cannot be detected in our samples, as the bands are overwhelmed by the amide I band ( $\nu$  [CONH]) of the parchment. The main spectral features of weld seem to be observed in the spectral region below approximately

TABLE 2 List of characteristic Raman bands detected for the chromophores in the red dye paint mock-ups and their tentative assignment

Madder lake Band (cm <sup>-1</sup> )	Cochineal lake			Brazilwood lake				
	Tentative assignment	Reference	Band (cm <sup>-1</sup> )	Assignment	Reference	Band (cm <sup>-1</sup> )	Assignment	Reference
400–611	Skeletal deformations	[19]	400–600	Skeletal deformations		764	$\gamma$ (C–O) + $\gamma$ (CH)	[44]
850–863	$\delta$ (C–H) + $\delta$ (C–O) <i>a,p</i>	[19,35]	814–820	$\delta$ (COH)	[22]	1006–1007	$\nu$ (C–C) + $\nu$ (C–O)	[44]
1007	$\nu$ (CC) + $\delta$ (CCC) <i>a</i>	[19,35]	851–857	$\delta$ Glu (CH <sub>2</sub> ) + $\delta$ (CCC)	[22]	1030–1036	$\nu$ (ring), breath	[44]
1030–1036	$\nu$ (CC) + $\delta$ (CH) <i>a,p</i>	[19,35]	978–983	$\rho$ (CH <sub>3</sub> ) + $\delta$ (CCC)	[22]	1167–1170	$\delta$ (CCH) + $\nu$ (C–C) <i>be</i>	[27]
1190–1201	$\nu$ (CC) + $\delta$ (CH) + $\delta$ (CCC) <i>a,p</i> / $\nu$ (CC) + $\delta$ (CH) <i>a,p</i>	[19,35]	1053–1062	$\nu$ (C–C), Glu + $\delta$ (COH), Glu	[22]	1238–1245	$\nu$ (C–O) + $\nu$ (C–C) <i>bi,be</i>	[27,44]
1245–1250	$\nu$ (CO) + $\nu$ (CC) <i>p</i>	[19]	1264–1274	$\nu$ (CC) + $\delta$ (COH), acid + $\delta$ (COH) + $\delta$ (CH), Glu	[22]	1272	$\nu$ (C–O) + $\nu$ (C–C) + $\delta$ (CH <sub>2</sub> ) <i>bi</i> / $\delta$ (C–C)	[27,44]
1294	$\nu$ (CO) + $\nu$ (CC) + $\delta$ (COH) + $\delta$ (CCC) <i>a,p</i>	[19,35]	1638–1640	$\nu$ (C–O) + $\nu$ (CC)	[22]	1294, 1310	$\nu$ (C–O) + $\nu$ (C–C) + $\delta$ (CH <sub>2</sub> ) <i>be,bi</i>	[44]
1452–1466	$\nu$ (CC) + $\delta$ (CH) + $\delta$ (CH) <i>a,p</i>	[19,71]	1736	$\nu$ (C=O), acid	[22]	1448–1450	$\nu$ (C=O) + $\delta$ (ring) + $\delta$ (COH) <i>be,bi</i>	[44]
1591	$\nu$ (CC) <i>a,p</i>	[19,35]				1562–1570	$\nu$ (C=C) <i>bi</i>	[44]
1634–1640	$\nu$ (C=O) <i>p</i>	[35]				1600	$\nu$ (C=O) <i>be</i>	[44]
						1610	$\nu$ (C=C) + $\nu$ (C=O) <i>be</i>	[44]

Abbreviations: *A*, alizarin; *p*, purpurin; *be*, brazilin; *bi*, brazilin; *Glu*, glucosidal function.

**TABLE 3** List of characteristic Raman bands detected for the chromophores in the yellow dye paint mock-ups and their tentative assignment

Band (cm <sup>-1</sup> )	Tentative assignment	Reference
682–689	$\delta$ (CC), ring deformation <i>l</i>	[26]
838–857	$\delta$ (CH) <i>l</i>	[26]
917–923	$\delta$ (COC) <i>ap l</i>	[26]
1000–1012	$\delta$ (CH) <i>l</i>	[26]
1124–1128	$\delta$ (CH) + $\delta$ (OH) <i>l</i>	[26]
1167–1178	$\delta$ (CH) <i>ap</i>	[26]
1245	$\delta$ (CH) + $\delta$ (OH) <i>ap</i>	[26]
1267–1272	$\nu$ (OH) <i>l</i>	[26]
1316	$\delta$ (CH) + $\delta$ (OH) <i>ap</i>	[26]
1404	$\delta$ (OH) <i>ap</i>	[26]
1448–1453	$\delta$ (OH) <i>ap</i>	[26]
1560	$\nu$ (C=O) <i>ap</i>	[26]
1585	$\nu$ (C=O) + $\delta$ (OH) <i>ap</i> / $\nu$ (C=C) <i>l</i>	[26]
1664–1669	$\nu$ (C=O) + $\nu$ (C=C) + $\delta$ (OH) <i>l</i>	[26]

Abbreviations: *l*, luteolin; *ap*, apigenin.

1400 cm<sup>-1</sup>. These can be attributed to  $\delta$  (CH) and  $\delta$  (OH) deformations,<sup>[26]</sup> whereas the intense features around 1000 and 900 cm<sup>-1</sup> are rather associated with ring stretching vibrations of the substituted benzene and the substituted benzopyran units, respectively.

### 3.2 | Identification of the binding agents

Lakes and pigments applied in painted artefacts are mixed with organic, viscous substances (binding agents) to form suspensions of chromatic particles and ensure their adhesion to the support.<sup>[73]</sup> The spectra presented in Figures 2 and 3 all originate from samples where gum Arabic—the exudate of *A. Senegal* trees consisting of glycoproteins and polysaccharides—was used as a binder. However, the Raman spectra of pictorial binders are prone to overlapping with those of the lake, because of their organic nature. In order to evaluate this possible interference, Raman spectra have been recorded of historical reconstructions of painted lakes prepared with different binding media. In Figure 4, the Raman spectrum of cochineal lake mixed with the chosen media is presented, namely gum Arabic, glair and egg yolk. The information on the binding media is summarised in Table 4; the Raman bands that are mentioned are present in Table 4 and were also detected in the Raman spectra of the other possible lake-binder mixtures: For instance, all lakes mixed with gum Arabic revealed characteristic

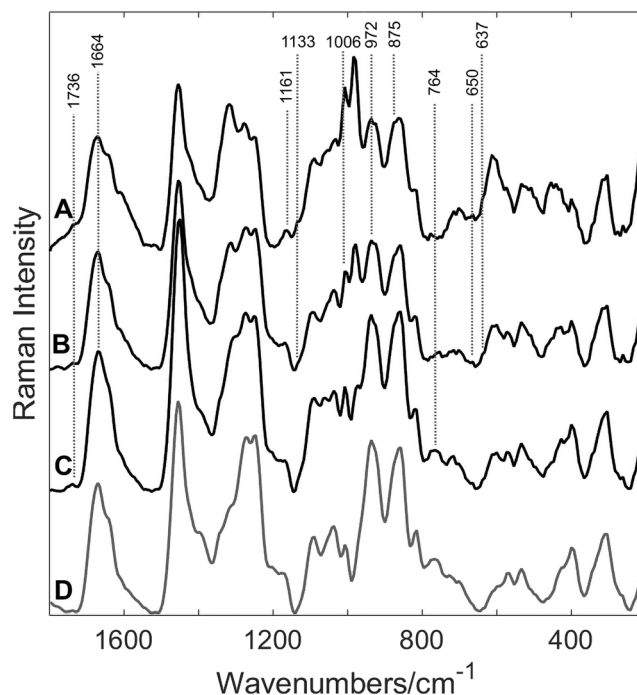


**FIGURE 4** Raman spectra of mock-ups of the same dye lake (cochineal lake, CL) mixed to different binders, all excited with 1064-nm laser, 10 accumulations, 30-s integration time and captured with the fibre-optic instrument: (A) CL + gum Arabic, (B) CL + egg white, (C) CL + egg yolk and (D) parchment support. Raman band positions (cm<sup>-1</sup>) are marked as discussed in the text.

doublets around 972–983 cm<sup>-1</sup> and 875–881 cm<sup>-1</sup>, both assigned to the  $\delta$  (COC) deformations of polysaccharides. At higher Raman wavenumbers, a weak Raman band was observed at approximately 1160 cm<sup>-1</sup>, which is related to the  $\nu$  (CC) or  $\nu$  (CO) stretching vibrations of saccharides<sup>[73]</sup> (Figure 4A).

The analysis of the lakes mixed with glair (denatured egg white) also showed a comparable response across the models (Figure 4B), corresponding to the bands arising from amide I and amide III modes as well as further stretching vibrations and other vibrational modes associated to the phenylalanine and tyrosine amino acids.<sup>[72,73]</sup> However, it should also be remarked that the parchment support consists of proteinaceous molecules, thus presenting highly similar Raman bands.

As for the analysis of the lakes with egg yolk, it might be characterised through a limited set of characteristic bands (Figure 4C). One is at 1006 cm<sup>-1</sup> associated with phenylalanine; another is the one at 765 cm<sup>-1</sup>, possibly related to the tryptophan fraction.<sup>[73,74]</sup> Finally, some weak bands are present at 1669 and 1736–1741 cm<sup>-1</sup>, arising from the  $\nu$  (C=O) mode of esters in fatty acids,<sup>[74]</sup> and can be observed at the high wavenumber edge of the amide I band of the parchment.

TABLE 4 List of characteristic Raman bands detected for gum Arabic, egg white and egg yolk and their tentative assignment

Gum Arabic			Egg white			Egg yolk		
Band (cm <sup>-1</sup> )	Tent. assign.	Ref.	Band (cm <sup>-1</sup> )	Tent. assign.	Ref.	Band (cm <sup>-1</sup> )	Tent. assign.	Ref.
875–881	δ (COC)	[72]	637	δ (ring)/ν (CS)	[73]	764	Trp	[72,73]
972–983	δ (COC)	[72]	650	δ (ring)/ν (CS)	[73]	1006		
1161	ν (CC)/ν (CO)	[72]	935	ρ (CH <sub>3</sub> ),	[73]	1664	ν (C=O)/ν (C=O), esters of f.a.	[72,73]
			1006	ν (CC), ar. ring breath	[73]	1736	ν (C=O), esters of fatty acids	[73]
			1133	ν (CC),	[72,73]			
			1167	ν (CC), Phe	[72,73]			

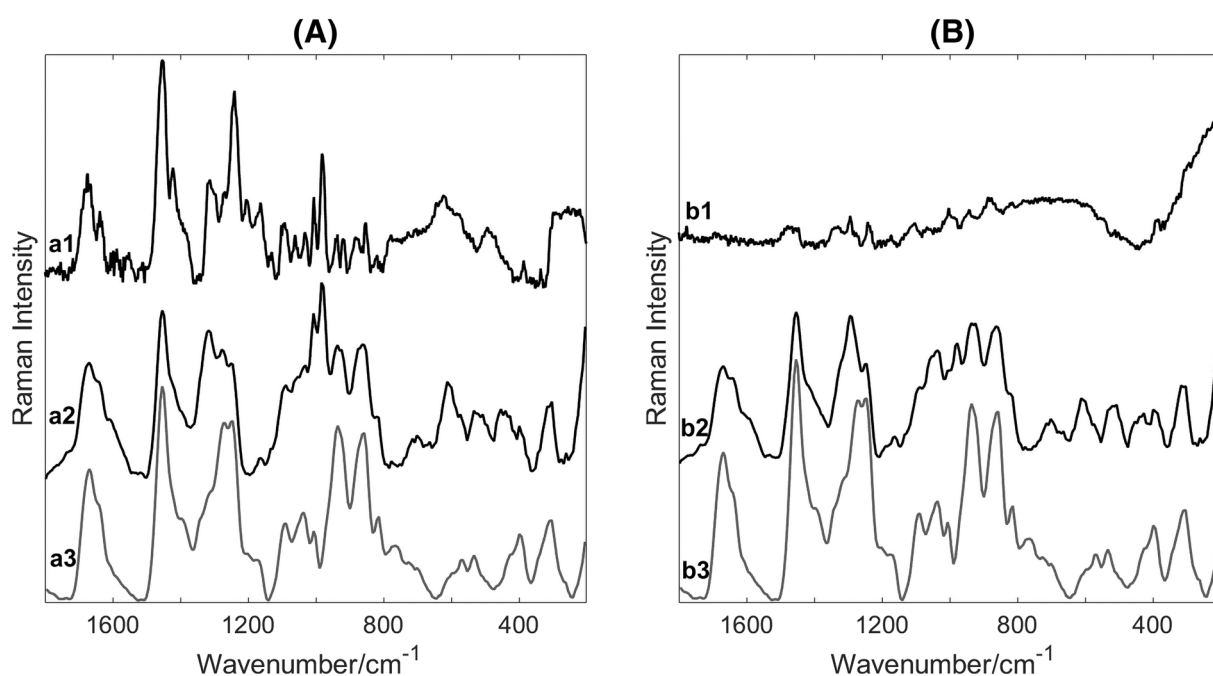


FIGURE 5 Spectra of the same mixture: (A) cochineal dye lake in gum Arabic, captured with the two instruments. The results are denoted as (a1) fibre-optic spectrum, all excited with 1064 nm laser; (a2) SSE spectrum, excited with lasers in the range 700–1100 nm; and (a3) parchment ground, analysed with the fibre-optic instrument. (B) Fibre-optic versus SSE spectra of madder lake in gum Arabic compared: (b1) fibre-optic spectrum, (b2) SSE spectrum and (b3) parchment ground

### 3.3 | Comparative assessment

At a close look, the Raman spectra of the same sample obtained from 1064-nm excitation with the two handheld instruments—the dispersive one and the one using the SSE algorithm—showed important differences. From these spectra, it seems that the instrument using the fibre-optic instrument picks up more spectral features originating from the parchment, whereas the parchment Raman bands are less dominant in the Raman spectra processed with the SSE algorithm (1064 nm). On the

other hand, it seems that the spectral quality between the spectrum from the fibre-optic device (Figure 5A) and the reconstructed SSE spectrum (Figure 5B) is significantly different. In the region with mainly skeletal vibrations (400–700 cm<sup>-1</sup>), the SSE algorithm suppresses most of the useful signal for all dye lakes, hampering the identification of these spectra in this range of Raman shifts. In fact, discrimination of the most characteristic vibrations reported for the individual chromophores is possible with dispersive near-infrared Raman spectroscopy, although these spectra appear quite noisy compared with pure



**TABLE 5** List of the calculated difference in band centres across the two portable instruments evaluated in this study, and reference values for the analysis of pure standards of pure chromophores with SERS and FTRS (values from<sup>[15,27,37,44,49]</sup>)

Parameter	Difference in energy (cm <sup>-1</sup> )		
	Madder lake	Cochineal lake	Brazilwood lake
Fibre-optic instrument vs SSE instrument	2.3–6.5 (± 2.3)		
Fibre-optic instrument vs SERS	7.8 ± 3.9	8.0 ± 4.0	4.1 ± 2.1
SSE instrument vs SERS	6.5 ± 3.3	10.3 ± 5.2	7.0 ± 3.5
Fibre-optic instrument vs FTRS	4.8 ± 2.4	18.0 ± 9.0	9.2 ± 4.6
SSE instrument vs FTRS	7.0 ± 3.5	17.6 ± 8.8	8.8 ± 4.4

standards (i.e. non-complexed dyes). At higher Raman shifts, the SSE algorithm amplifies several bands for most lake mixtures, except for madder lake (Figure 5B): In this case, the portable instrument fails at detecting those falling between 1200 and 1400 cm<sup>-1</sup> as well as between 1500 and 1600 cm<sup>-1</sup>. However, concerning the better signal-to-noise ratio of the spectra obtained with the Bruker Bravo (SSE) instrument, some remarks should be made. Firstly, the laser power at the sample is unknown. No visual damage to the paint surface was observed, but working with cultural heritage objects, one should pay sufficient attention to this issue. Moreover, the spectrum that is obtained from this instrument is a reconstruction, based on the recording of six different spectra, excited with two different lasers (785 and 853 nm). During the mathematical reconstruction of the baseline correction, inherently, some smoothing is applied, which results in a seemingly better spectral quality.

Further differences arose in terms of band shifts between the spectra of the two devices. Differences in Raman band positions are observed in most of the cases, with shifts ranging between approximately 2 and 6.5 cm<sup>-1</sup>. These shifts seem to be random and do not seem to obey some trends over the spectral range. Next to random variations, laser-induced degradation could be a possible reason for this observation. Moreover, the band positions as recorded in this study differ significantly from the band positions reported in the literature, based on SERS and FT-Raman spectroscopy (Table 5).

Looking at Table 5, it can be seen that the shifts are not consistent for all red dyes in the study. It should be noted that shifts can be caused not only by spectroscopic reasons (e.g. calibration) but also that different samples are considered, having different extraction and preparation procedures from those followed in the cited references. The complexation, or more generally, the formation of a dye-binder network, can have a strong effect on the Raman spectra. Moreover, when comparing with SERS spectra, also because of the interaction with the

metal, changes in band position can occur. Finally, the mentioned SERS and FT-Raman spectroscopy studies were performed on dye lakes in either their extracted or pure form, thus neglecting the effects arising from the creation of such a complex system as a paint model.

## 4 | CONCLUSIONS

This paper illustrates the test of the applicability of portable Raman instruments for the analysis of historic dye lakes. For the study, two commercial instruments using two different acquisition and data processing technologies were considered and their analytical potential was tested on a set of laboratory reproductions. The models studied were mock-ups of historically accurate paint mixtures prepared according to the instructions of mediaeval technical texts (12th–16th century) including a number of common lakes (madder lake, cochineal lake, brazilwood lake and weld lake) mixed with binding agents of different chemical classes (polysaccharide, protein, mixed protein-fatty acids). The acquired data showed that the discrimination of the different lakes is possible, based on certain marker bands. Moreover, this study showed that the spectra acquired with the two instruments bear different spectral content.

## ACKNOWLEDGEMENTS

The research was supported by the Portuguese Foundation for Science and Technology (FCT) by National Funds under the R&D projects and units *Cistercian Horizons* (PTDC/ART-HIS/29522/2017), *HERCULES Laboratory* (UIDP/04449/2020 and UIDB/04449/2020) and Norma Transitória (DL 57/2016/CP1372/CT0012).

## AUTHOR CONTRIBUTION STATEMENT

All authors contributed to the design and implementation of the research, to the analysis of the results and to the writing of the manuscript.

## DATA AVAILABILITY STATEMENT

The data that support the findings of this study are available from the corresponding author upon reasonable request.

## ORCID

Silvia Bottura-Scardina  <https://orcid.org/0000-0002-3566-5921>

Peter Vandenabeele  <https://orcid.org/0000-0001-5285-9835>

Catarina Miguel  <https://orcid.org/0000-0002-4722-8067>

António Candeias  <https://orcid.org/0000-0002-4912-5061>

## REFERENCES

- [1] F. Brunello, *De arte illuminandi*, Neri Pozza, Vicenza **1975**.
- [2] C. Clementi, B. Doherty, P. L. Gentili, C. Miliani, A. Romani, B. G. Brunetti, A. Sgamellotti, *Appl. Phys. A: Mater. Sci. Process.* **2008**, *92*, 25.
- [3] C. J. Herringham, *The book of the art of Cennino Cennini*, G. Allen & Unwin, London **1899**.
- [4] C. Grazia, C. Clementi, C. Miliani, A. Romani, *Photochem. Photobiol. Sci.* **2011**, *10*, 1249.
- [5] K. Solymosi, N. Latruffe, A. Morant-Manceau, B. Schoefs, in *Colour additives for foods and beverages*, (Ed: M. J. Scotter), Elsevier, Amsterdam **2015** 3.
- [6] K. Wongsooksin, S. Rattanaphani, M. Tangsathitkulchai, V. Rattanaphani, J. B. Bremner, *Suranaree J. Sci. Technol.* **2008**, *15*, 159.
- [7] T. Vitorino, A. Casini, C. Cucci, M. J. Melo, M. Picollo, L. Stefani, *Appl. Phys. A: Mater. Sci. Process.* **2015**, *121*, 891.
- [8] S. Fletcher, L. Glinsman, D. Doris, *Studies in the History of Art* **2009**, *75*, 276.
- [9] O. Hahn, D. Oltrogge, H. Bevers, *Archaeometry* **2004**, *46*, 273.
- [10] M. J. Melo, V. Otero, T. Vitorino, R. Araújo, V. S. F. Muralha, A. Lemos, M. Picollo, *Appl. Spectrosc.* **2014**, *68*, 434.
- [11] P. Nabais, M. J. Melo, J. A. Lopes, T. Vitorino, A. Neves, R. Rita, *Herit. Sci.* **2018**, *6*, 13.
- [12] T. Vitorino, *A closer look at Brazilwood and its Lake pigments*, Universidade NOVA de Lisboa, Lisbon **2012**.
- [13] C. Muehlethaler, K. Ng, L. Gueissaz, M. Leona, J. R. Lombardi, *Dyes Pigm.* **2017**, *137*, 539.
- [14] A. Romani, C. Clementi, C. Miliani, G. Favaro, *Acc. Chem. Res.* **2010**, *43*, 837.
- [15] M. Leona, J. Stenger, E. Ferloni, *J. Raman Spectrosc.* **2006**, *37*, 981.
- [16] G. Favaro, C. Miliani, A. Romani, M. Vagnini, *J. Chem. Soc., Perkin Trans.* **2002**, *2*, 192.
- [17] C. Miliani, A. Romani, G. Favaro, *J. Phys. Org. Chem.* **2000**, *13*, 141.
- [18] A. Baran, B. Wrzosek, J. Bukowska, L. M. Proniewicz, M. Baranska, *J. Raman Spectrosc.* **2009**, *40*, 436.
- [19] M. V. Cañamares, J. V. Garcia-Ramos, C. Domingo, S. Sanchez-Cortes, *J. Raman Spectrosc.* **2004**, *35*, 921.
- [20] K. Retko, P. Ropret, R. C. Korošec, S. Sanchez-Cortes, M. V. Cañamares, *J. Raman Spectrosc.* **2018**, *49*, 1288.
- [21] I. T. Shadi, B. Z. Chowdhry, M. J. Snowden, R. Withnall, *J. Raman Spectrosc.* **2004**, *35*, 800.
- [22] M. V. Cañamares, J. V. Garcia-Ramos, C. Domingo, S. Sanchez-Cortes, *Vib. Spectrosc.* **2006**, *40*, 161.
- [23] M. V. Cañamares, M. Leona, *J. Raman Spectrosc.* **2007**, *38*, 1259.
- [24] Z. Jurasekova, J. V. Garcia-Ramos, C. Domingo, S. Sanchez-Cortes, *J. Raman Spectrosc.* **2006**, *37*, 1239.
- [25] T. Teslova, C. Corredor, R. Livingstone, T. Spataru, R. L. Birke, J. R. Lombardi, M. V. Cañamares, M. Leona, *J. Raman Spectrosc.* **2007**, *38*, 802.
- [26] C. Corredor, T. Teslova, M. V. Cañamares, Z. J. Chen, J. Zhang, J. R. Lombardi, M. Leona, *Vib. Spectrosc.* **2009**, *49*, 190.
- [27] L. F. C. de Oliveira, H. Edwards, E. S. Velozo, M. Nesbitt, *Vib. Spectrosc.* **2002**, *28*, 243.
- [28] H. G. M. Edwards, L. F. C. de Oliveira, M. Nesbitt, *Analyst* **2003**, *128*, 82.
- [29] S. Bruni, V. Guglielmi, F. Pozzi, *J. Raman Spectrosc.* **2011**, *42*, 1267.
- [30] E. Casanova-González, M. A. Garcia-Bucio, J. L. Ruvalcaba-Sil, V. Santos-Vasquez, B. Esquivel, T. Falcón, E. Arroyo, S. Zetina, M. L. Roldán, C. Domingo, *J. Raman Spectrosc.* **2012**, *43*, 1551.
- [31] A. Idone, M. Gulmini, A.-I. Henry, F. Casadio, L. Chang, L. Appolonia, R. P. Van Duyne, B. C. Shah, *Analyst* **2013**, *138*, 5895.
- [32] E. M. Angelin, S. França de Sá, M. Picollo, A. Nevin, M. E. Callapez, M. J. Melo, *J. Raman Spectrosc.* **2021**, *52*, 145.
- [33] F. Marte, V. P. Careaga, N. Mastrangelo, D. L. A. de Faria, M. S. Maier, *J. Raman Spectrosc.* **2013**, *45*, 1046.
- [34] I. Osticioli, M. Pagliai, D. Comelli, V. Schettino, A. Nevin, *Spectrochim. Acta, Part a* **2019**, *222*, 1386, 117273.
- [35] F. Rosi, M. Paolantoni, C. Clementi, B. Doherty, C. Miliani, B. Brunetti, A. Sgamellotti, *J. Raman Spectrosc.* **2010**, *41*, 452.
- [36] I. Osticioli, A. Zoppi, E. M. Castellucci, *J. Raman Spectrosc.* **2006**, *37*, 974.
- [37] L. Burgio, R. J. H. Clark, *Spectrochim. Acta, Part a* **2001**, *57*, 1491.
- [38] M. Leona, *PNAS* **2009**, *106*, 14757 147571.
- [39] R. Withnall, I.T. Shadi, B.Z. Chowdhry, in *Raman spectroscopy in archaeology and art history* (Eds: H.G.M. Edwards, J.M. Chalmers), The Royal Society of Chemistry, Cambridge, **2005**, pp. 152–168.
- [40] F. Casadio, M. Leona, J. R. Lombardi, R. Van Duyne, *Acc. Chem. Res.* **2010**, *43*, 782.
- [41] K. Chen, M. Leona, K. C. Vo-Dinh, F. Yan, M. B. Wabuyele, T. Vo-Dinh, *J. Raman Spectrosc.* **2006**, *37*, 520.
- [42] Z. Jurasekova, C. Domingo, J. V. Garcia-Ramos, S. Sanchez-Cortes, *J. Raman Spectrosc.* **2008**, *39*, 1309.
- [43] F. Pozzi, J. R. Lombardi, S. Bruni, M. Leona, *Anal. Chem.* **2012**, *84*, 3751.
- [44] A. V. Whitney, R. P. Van Duyne, F. Casadio, *J. Raman Spectrosc.* **2006**, *37*, 993.
- [45] L. H. Oakley, S. A. Dinehart, S. A. Svoboda, K. L. Wustholz, *Anal. Chem.* **2011**, *83*, 3986.
- [46] K. Retko, L. Legan, P. Ropret, *J. Raman Spectrosc.* **2021**, *52*, 130.
- [47] C. L. Brosseau, K. S. Rayner, F. Casadio, C. M. Grzywacz, R. P. Van Duyne, *Anal. Chem.* **2009**, *81*, 7443.
- [48] H. E. Mayhew, D. M. Fabian, S. A. Svoboda, K. L. Wustholz, *Analyst* **2013**, *138*, 4493.

- [49] L. H. Oakley, D. M. Fabian, H. E. Mayhew, S. A. Svoboda, K. L. Wustholz, *Anal. Chem.* **2012**, *84*, 8006.
- [50] M. M. Eisnor, K. E. R. McLeod, S. Bindesri, S. A. Svoboda, K. L. Wustholz, C. L. Brosseau, *Phys. Chem.* **2022**, *24*, 347.
- [51] P. Vandenaabeele, H. G. M. Edwards, J. Jehlička, *Chem. Soc. Rev.* **2014**, *43*, 2628.
- [52] D. Bersani, C. Conti, P. Matousek, F. Pozzi, P. Vandenaabeele, *Anal. Methods* **2016**, *8*, 8395.
- [53] A. Deneckere, F.-P. Hocquet, A. Born, P. Klein, S. Rakkaa, S. Lycke, K. De Langhe, M. Martens, D. Strivay, P. Vandenaabeele, L. Moens, *J. Raman Spectrosc.* **2010**, *41*, 1500.
- [54] M. Irazola, M. Olivares, K. Castro, M. Maguregui, I. Martínez-Arkarazo, J. M. Madariaga, *J. Raman Spectrosc.* **2012**, *43*, 1676.
- [55] R. Mulholland, D. Howell, A. Beeby, C. E. Nicholson, K. Domoney, *Herit. Sci.* **2017**, *5*, 43.
- [56] A. Rousaki, P. Vandenaabeele, *J. Raman Spectrosc.* **2021**, *52*, 2178.
- [57] P. Vandenaabeele, K. Lambert, S. Matthys, W. Schudel, A. Bergmans, L. Moens, *Anal. Bioanal. Chem.* **2005**, *383*, 707.
- [58] P. Colomban, A. Tournié, *J. Cult. Herit.* **2007**, *8*, 242.
- [59] P. Ricciardi, P. Colomban, A. Tournié, V. Milande, *J. Raman Spectrosc.* **2009**, *40*, 604.
- [60] P. Colomban, L. Arberet, B. Kırmızı, *Ceram. Int.* **2017**, *43*, 10158.
- [61] P. Colomban, T.-A. Lu, V. Milande, *Ceram. Int.* **2018**, *44*, 9018.
- [62] P. Colomban, B. Kırmızı, C. Gougeon, M. Gironda, C. Cardinal, *J. Cult. Herit.* **2020**, *44*, 1.
- [63] F. Koleini, P. Colomban, I. Pikirayi, *J. Archaeol. Sci. Rep.* **2020**, *29*, 102183.
- [64] D. de Waal, *J. Raman Spectrosc.* **2009**, *40*, 2162.
- [65] D. Bersani, P. P. Lottici, F. Vignali, G. Zanichelli, *J. Raman Spectrosc.* **2006**, *37*, 1012.
- [66] D. C. Smith, *Spectrochim. Acta, Part a* **2003**, *59*, 2353.
- [67] J. B. Cooper, M. Abdelkader, K. L. Wise, *Appl. Spectrosc.* **2013**, *67*, 973.
- [68] C. Conti, A. Botteon, M. Bertasa, C. Colombo, M. Realini, D. Sali, *Analyst* **2016**, *141*, 4599.
- [69] B. Campanella, E. Grifoni, M. Hidalgo, S. Legnaioli, G. Lorenzetti, S. Pagnotta, F. Poggialini, L. Ripoll-Seguer, V. Palleschi, *J. Cult. Herit.* **2018**, *33*, 208.
- [70] A. Chieli, J. Sanyova, B. Doherty, B. G. Brunetti, C. Miliani, *Spectrochim. Acta, Part a* **2016**, *162*, 86.
- [71] D. Hutsebaut, P. Vandenaabeele, L. Moens, *Analyst* **2005**, *130*, 1204.
- [72] S. Murcia-Mascarós, C. Domingo, S. Sanchez-Cortes, M. V. Cañameres, J. V. Garcia-Ramos, *J. Raman Spectrosc.* **2005**, *36*, 420.
- [73] P. Vandenaabeele, B. Wehling, L. Moens, H. G. M. Edwards, M. De Reu, G. Van Hooydonk, *Anal. Chim. Acta* **2000**, *407*, 261.
- [74] I. Osticioli, A. Nevin, D. Anglos, A. Burnstock, S. Cather, M. Becucci, C. Fotakis, E. Castellucci, *J. Raman Spectrosc.* **2008**, *39*, 993.
- [75] M. Pagliai, I. Osticioli, A. Nevin, S. Siano, G. Cardini, V. Schettino, *J. Raman Spectrosc.* **2017**, *49*, 668.

**How to cite this article:** S. Bottura-Scardina, P. Vandenaabeele, C. Miguel, A. Candeias, *J Raman Spectrosc* **2023**, *54*(11), 1303. <https://doi.org/10.1002/jrs.6501>